

Preparation, characterization and thermal behavior of poly(vinyl alcohol)/organic montmorillonite nanocomposites through solid-state shear pan-milling

Cuiying Li · Wei Zhang · Bo Zhao ·
Mei Liang · Canhui Lu

Received: 31 October 2009 / Accepted: 23 July 2010 / Published online: 14 August 2010
© Akadémiai Kiadó, Budapest, Hungary 2010

Abstract In this study, the solid-state shear pan-milling was employed to prepare a series of polymer/layered silicate (PLS) nanocomposites. During the process of pan-milling at ambient temperature, poly(vinyl alcohol)/organic montmorillonite (PVA/OMMT) can be effectively pulverized, resulting in coexistence of intercalated and exfoliated OMMT layers. The obtained PLS nanocomposites were characterized by X-ray diffraction (XRD) and transmission electron microscopy (TEM). TEM analysis indicated that OMMT dispersed homogeneously in PVA matrix and XRD results illustrated that pan-milling had an obvious effect on increase in the interlayer spacing of OMMT, and resulted in coexistence of intercalated and exfoliated OMMT layers formed. Thermal gravimetric analysis showed that thermal stability of PVA was improved owing to the incorporation of OMMT. Thermal decomposition kinetics of PVA/OMMT nanocomposites with different milling cycles of OMMT was also studied. Two types of OMMT are chosen to compare the effect of hydrophilicity of OMMT on PVA/OMMT nanocomposites.

Keywords Solid-state shear pan-milling · Poly(vinyl alcohol) · Organic montmorillonite · Thermal behavior · Nanocomposites

Introduction

Over the last few years, polymer/layered silicate (PLS) nanocomposites have attracted more and more attentions due to their unique properties resulting from the nano-scale structures [1–7]. These PLS nanocomposites often exhibit remarkably improved properties as compared to neat polymers, showing high storage modulus, increased tensile flexural properties, heat distortion temperature and the biodegradability rate of biodegradable polymers [2–4, 7–10]. The extremely high surface area of nano-components in composites mainly contributes to their property enhancements, because it facilitates the formation of a large interphase in composites, thus creating a strong interaction between matrix and fillers even at a low filler loading.

It is well known that the dispersion quality of nanoparticles in polymer matrix directly influences the final properties of composites. On the basis of the strength of PLS nanocomposites, Ray et al. [8] have defined three types of nanocomposites: *intercalated nanocomposites*, *flocculated nanocomposites*, and *exfoliated nanocomposites*. Most researchers believe that a completely exfoliated structure of layered silicate with homogeneous dispersing state in matrix is the ultimate target for better overall properties due to the high aspect ratio of single-clay layers and the nanometer filler thickness being comparable to the scale of the polymer chain structure. The preparative methods of PLS are generally categorized into three main groups according to the starting materials and processing techniques: intercalation of polymer or pre-polymer from solution, in situ intercalative polymerization method, and melt intercalation method [2–4, 7–9]. From the view point of manufacturing efficiency and environmental concern, the last method has obvious advantages over the other two

C. Li · W. Zhang · B. Zhao · M. Liang · C. Lu (✉)
State Key Laboratory of Polymer Materials Engineering,
Polymer Research Institute, Sichuan University, Chengdu,
Sichuan 610065, People's Republic of China
e-mail: canhuilu@263.net

which require complicated fabricating procedures with toxic solvents. However, for this method, the ideal intercalated or exfoliated structure cannot be satisfactorily achieved due to the high viscosity of polymer melt as well as the strong agglomerating tendency of nanoparticles. Besides, for its manufacturing process, a mixture of PLS must be heated to the temperature above the softening point of the polymer [3]. Therefore, it is quite difficult to apply this technique to the preparation of composite materials containing polymer matrix whose decomposition temperature and melting temperature are close, e.g., poly(vinyl alcohol) (PVA).

Gao et al. [11] reported the first approach to fabricate polymer/clay nanocomposites based on intercalation in solid phase. The expansion of interlayer distance of either hydrophilic layered-silicate or organophilic clay in a polymer matrix can be achieved simply by blending and compressing the solid mixture. Recently, Lu and Pan [12] realized a fine dispersion of nano-SiO_x particles in PPS simply by pulverizing of the mixture through a ball-milling technique. However, for the ball mill and most other milling equipments, the high-energy consumption and low efficiency of the preparation of polymer powder are unavoidable, limiting this promising technology in a laboratory scale [13]. A novel pan-type mill was previously invented by our lab, as shown in Fig. 1. Figure 2 illustrates the detailed structure of its key part, the inlaid pan. Theoretical analysis demonstrates that this equipment has excellent pulverizing and dispersing effects on polymeric materials owing to the ingenious design derived from the traditional Chinese stone-mill. Functioning like a pair of three-dimensional scissors, it can exert a strong squeezing force on materials between the pans in both radial and tangential directions. In our previous work, using the pan-type mill, we have realized pulverization, dispersion, activation, and mechanochemical reactions of polymer materials [14–16]. Most recently, the intercalation and exfoliation of talc as well as vermiculite layer in PP as matrix were successfully achieved by using the pan-mill equipment in solid state. Improved comprehensive properties such as thermal properties, crystallization properties, and mechanical properties were exhibited for these products [17–23].

As a pioneering work, the pan-milling technique was used in this study to achieve intercalated and exfoliated OMMT as well as the fine dispersion of nanoparticles into the polymer matrix in solid state. It must be of both scientific and commercial interest because this method is time and energy saving, as well as no hazardous solvent is needed, compared with the conventional preparation of PVA-clay nanocomposites by solution dispersion technique or in situ polymerization in recent publication [3, 7, 13, 24–26]. The neat PVA and co-milled PVA/organic



Fig. 1 Digital photograph of the pan-mill type mechanochemical reactor

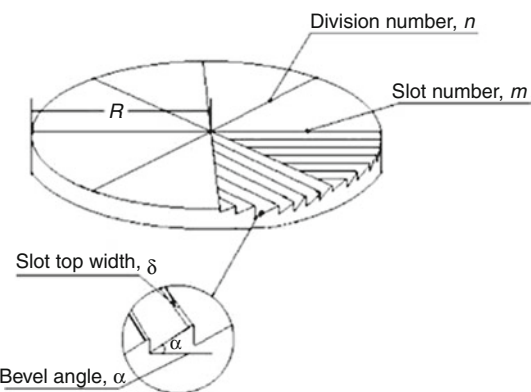


Fig. 2 Schematic diagram of an inlaid mill pan

montmorillonite (OMMT) powder were characterized by XRD and transmission electron microscopy (TEM) to indicate the intercalated and exfoliated silicate layers and how these layers disperse in PVA matrix. The thermal stability of as-obtained composites was investigated by TG. Their thermal decomposition kinetics was discussed, to the best of our knowledge, for the first time by using Kissinger method and Ozawa method for this system. Furthermore, two kinds of OMMT (namely, OMMT1 and OMMT2, different in hydrophilicity) were used in our study to compare the effect of hydrophilic on increasing of interlayer spacing of OMMT and improvement of thermal stability.

Experiment section

Materials

PVA 1799 (degree of polymerization 1750 \pm 50, degree of alcoholysis of 99%) was provided by SINOPEC Sichuan Vinylon Works, China. Two types of organic montmorillonite (grade: DK4 and DK1N) were purchased from Zhejiang Chemical Plant, China. Those main component was Na-montmorillonite (MMT) organically modified by dioctadecyl dimethyl ammonium bromide. They were defined as OMMT1 and OMMT2, respectively, the content of organic group in OMMT1 is smaller than that of OMMT2, and show hydrophilic property.

Preparation of PVA/OMMT nanocomposites

Pristine PVA was washed several times using deionized water until a pH of 7 was achieved, then dried in oven at 60 °C to a constant mass. Then, the mixture of PVA and OMMT (mass ratio: 80/20) was fed into the inlet of the

pan-mill equipment which was set in the front of the static pan. Milled powder of PVA/OMMT was discharged from the brim of the pans, and then collected from the outlet for the next pan-milling cycle. The whole milling process was controlled by the rotating speed 40 rpm and the heat generated during milling was taken away by running water so that the milling pans kept ambient temperature during the whole process. We defined mixture of PVA and OMMT of different milling cycle as PVA/OMMT-20, PVA/OMMT-40, and PVA/OMMT-60, respectively.

Characterization

X-ray diffraction (XRD) data were collected on a Philips X'Pert X-diffractometer, using Cu K α radiation at $\lambda = 0.1540$ nm (40 kV, 40 mA), diffraction spectra were obtained over a 2θ range of 2–10° with a step interval of 0.02°. The samples were compacted to small mats for measurements. The interlayer distance of OMMT in composites was calculated from the (001) peak by using Bragg equation: $2d\sin\theta = \lambda$, where λ is the wavelength. Thermal

Fig. 3 XRD patterns of PVA/OMMT. Left PVA/OMMT1; right PVA/OMMT2 (*a* OMMT, *b* PVA/OMMT-20, *c* PVA/OMMT-40, *d* PVA/OMMT-60)

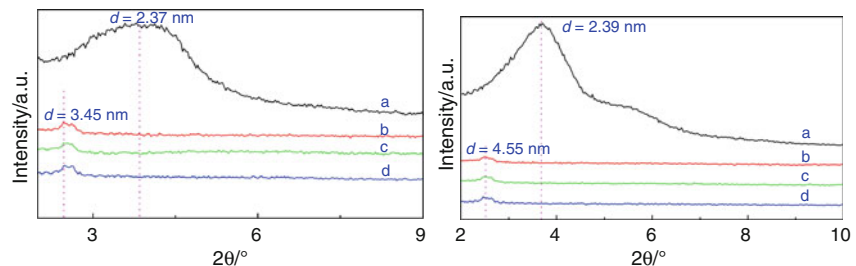
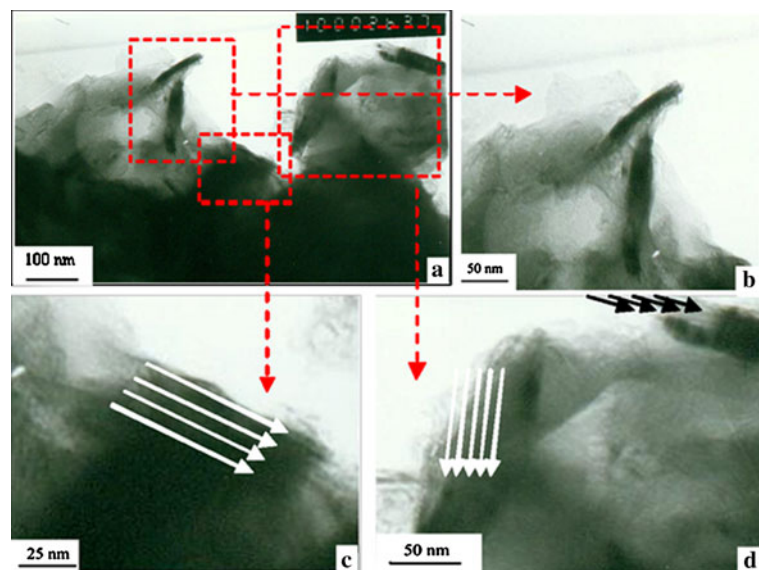


Fig. 4 TEM photos of PVA/OMMT1 milled for 60 pan-milling cycles



gravimetric (TG) analysis and derivative thermogravimetric (DTG) analysis were conducted on TA-2000 analyzer (TG Instrument). Sample of about 5 mg was placed in an open alumina crucible. Temperature programs for scanning were from room temperature to 873 K at a heating rate of 20 K min⁻¹. The measurements were operated under a nitrogen purge (100 mL min⁻¹). The morphology of mixture after specific milling cycles was observed under a TEM (JEOL JEM-100CX, Japan). The powder of mixture was dispersed in alcohol with ultrasonic, and specimen were prepared and then observed at an acceleration voltage of 80 kV.

Structural characterization

XRD measurements

XRD patterns of pristine OMMT and composite powder treated by the pan-mill are shown in Fig. 3. In Fig. 3 left, the powder XRD patterns show diffraction peaks in $2\theta = 4^\circ$ as opposed to the diffraction peak at $2\theta = 2.5^\circ$ after pan-milling for 20 cycles. Figure 3 right shows similar tendency after pan-milling for 20 cycles, the interlayer spacing of OMMT2 increases from 2.39 to 4.55 nm. Due to the intercalation of PVA chains into the interlayer space of OMMT, a new basal reflection corresponding to the larger gallery height appears [3]. The slight shift of the XRD peak to lower angle indicates the presence of a hybrid structure consisting of partially exfoliated or intercalated OMMT [27]. The intensity of the peak decreases after co-milling with PVA, which could also be the result of a partial exfoliation of layered silicates [28, 29]. However, the intensity and position of the peak keep almost stable with continued milling process after 20 cycles of pan-milling. This phenomenon may be the result of agglomeration of PVA micro-particles after certain cycles of pan-milling, which prevents OMMT from further exfoliation.

Transmission electron microscopy

Solid-state pan-milling offers fairly strong squeezing, shear, and friction forces on the milled materials, thus provide an appropriate stress field to delaminate the stacked structure. The co-milled materials will be pulverized, well mixed, and embedded into each other. The PVA chain diffusion into galleries of OMMT layers was accomplished during pan-milling process. In order to further illustrate the composite structures, the morphology of composites was observed by TEM. Figures 4 and 5 show the TEM images of PVA/OMMT1 and PVA/OMMT2, respectively. Both samples were treated by pan-milling of 60 cycles. The dark entities are the cross sections of intercalated OMMT layers [10]. Figure 4 shows that



Fig. 5 TEM photos of PVA/OMMT2 milled for 60 pan-milling cycles

OMMT has been exfoliated partly in PVA matrix, and an intercalated structure has been produced. In Fig. 4b, which is a locally magnified image, a number of well-dispersed partially exfoliated OMMT nano-platelets with length about 100 nm and thickness far below 100 nm can be observed obviously. Figure 4c, d shows that the OMMT particles on the matrix surface consist of OMMT layers exfoliated in a different degree. Un-exfoliated stacking OMMT decreased, some intercalated stack could be

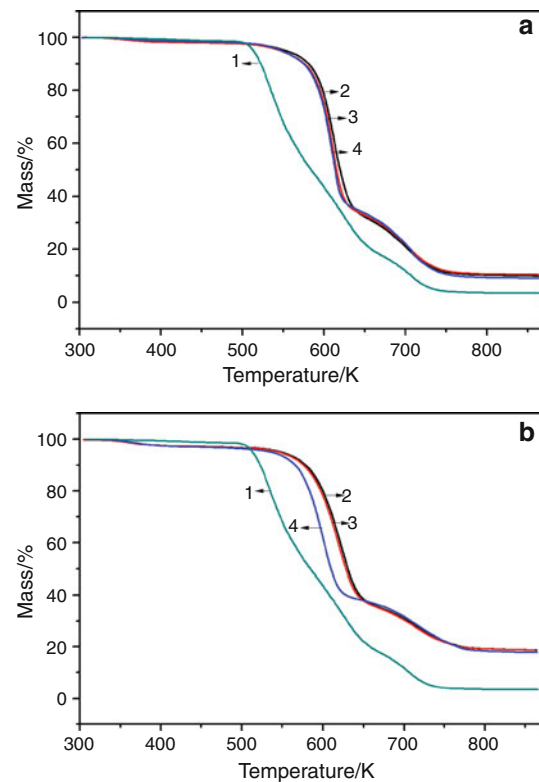


Fig. 6 **a** TG patterns of PVA/OMMT1 (1 PVA, 2 PVA/OMMT-20, 3 PVA/OMMT-40, 4 PVA/OMMT-60). **b** TG patterns of PVA/OMMT2 (1 PVA, 2 PVA/OMMT-20, 3 PVA/OMMT-40, 4 PVA/OMMT-60)

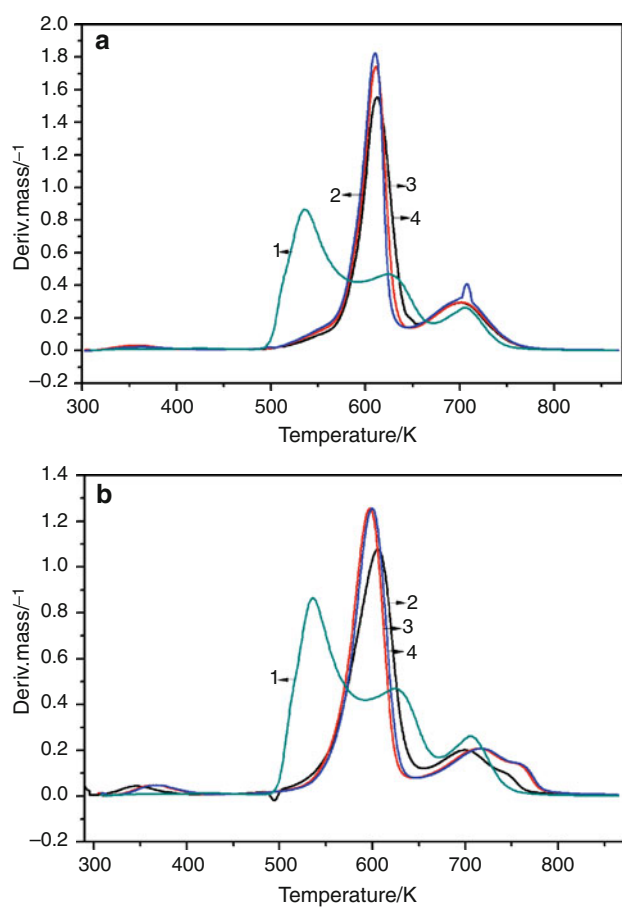


Fig. 7 **a** DTG patterns of PVA/OMMT1 (1 PVA, 2 PVA/OMMT-20, 3 PVA/OMMT-40, 4 PVA/OMMT-60), T_{p1} is the temperature at the highest weight loss peak. **b** DTG patterns of PVA/OMMT2 (1 PVA, 2 PVA/OMMT-20, 3 PVA/OMMT-40, 4 PVA/OMMT-60), T_{p1} is the temperature at the highest weight loss peak

Table 1 Properties of thermal degradation of PVA and PVA/OMMT with different pan-milling cycles

Sample	T_f^a /K	T_{p1}^b /K	DTG c_1 /mass/% K ⁻¹	Mass loss/%
PVA	488.1	573.2	0.82	78.4
PVA/OMMT1-20	589.9	612.6	1.55	60.9
PVA/OMMT1-40	589.2	611.2	1.74	57.9
PVA/OMMT1-60	592.0	610.2	1.79	55.7
PVA/OMMT2-20	607.1	636.9	1.46	51.8
PVA/OMMT2-40	604.4	634.8	1.54	49.0
PVA/OMMT2-60	603.1	632.7	1.54	50.7

^a The onset decomposition temperature

^b Temperature at the highest mass loss peak

^c Mass loss rate at T_{p1}

identified. Figure 5 shows that partly exfoliated OMMT layers exist in the nanocomposite powder both XRD and TEM consistently show that solid-state pan-milling of PVA

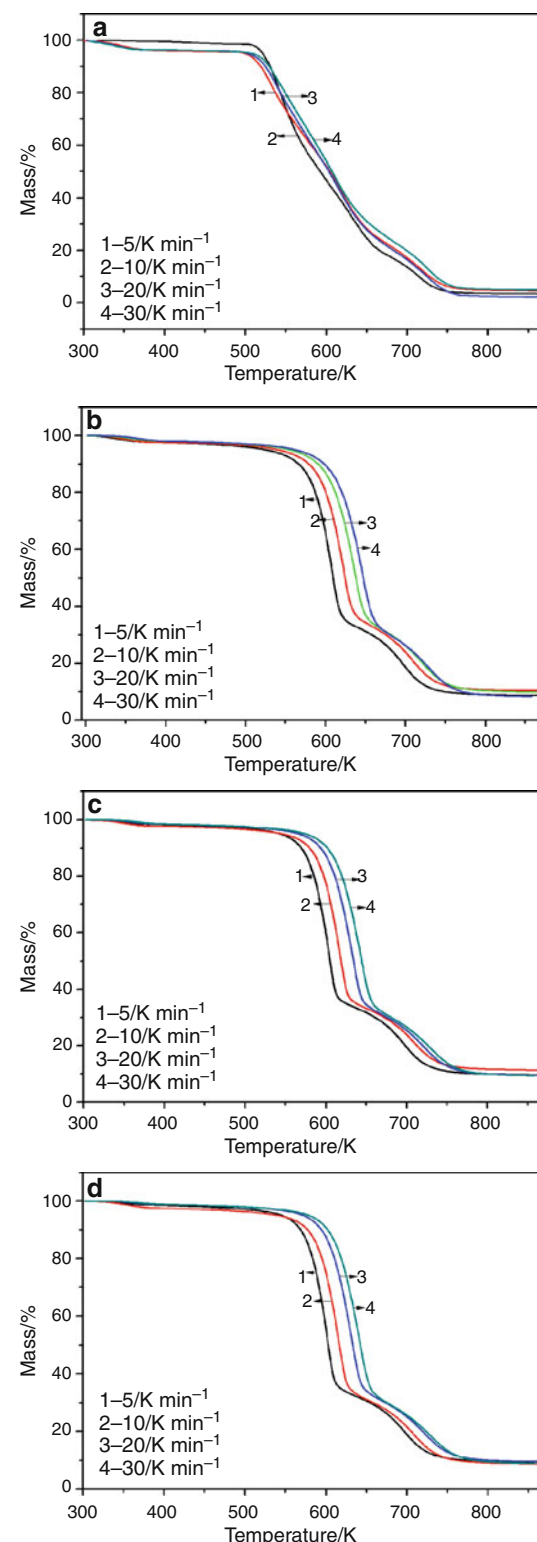


Fig. 8 TG patterns of **a** PVA, **b** PVA/OMMT2-20, **c** PVA/OMMT2-40, **d** PVA/OMMT2-60 nanocomposites at different heating rates

in the presence of OMMT leads to nanocomposites materials with a hybrid structure where both intercalated and exfoliated silicate layers coexist in considerable ratios.

Thermal analysis

The thermal stability of polymeric materials is usually studied by TG analysis [6]. Figure 6 shows the TG curves from 300 to 873 K of all samples. There is an evident shift of thermal decomposition temperature from pristine PVA to co-milled PVA/OMMT composites powder. The thermal decomposition of co-milled powder shifts toward higher temperature range as compared to that of PVA. All curves show slight mass loss at 373 K, probably because of evaporation of water. The starting decomposition temperature of PVA is 515.1 K, whereas the starting decomposition temperature of co-milled PVA/OMMT1 powder increased to 583.2 K, about 70 K higher than that of pristine PVA. This value for co-milled PVA/OMMT2 powder increased even higher, to nearly 603.2 K. DTG curves of co-milled powder of different cycles show two mass loss peaks in the temperature range from 473 to 773 K. However, three mass loss peaks were observed on the DTG curve of PVA. The first mass loss peak is at 537.2 K for PVA. After being co-milled with OMMT, first mass loss peak of the PVA/OMMT1 powder increased to about 613.2 K and that of PVA/OMMT2 powder is near 633.2 K. At the first mass loss peak, mass loss percentage is 78.4, 55.7, and 50.7% for pristine PVA, PVA/OMMT1, and PVA/OMMT2, respectively (Fig. 7). The relative data are listed in Table 1. In PVA/OMMT nanocomposites obtained by pan-milling, OMMT layers, which disperse as nanometer grade elements in PVA matrix, will hinder the movement of PVA molecular chain as well as the gas diffusion from inside of materials; therefore, thermal decomposition process is postponed, and their thermal stability can be improved. It is also worth noting that the thermal stability of PVA/OMMT2 is better than that of PVA/OMMT1.

Thermal decomposition kinetics study of PVA/OMMT nanocomposites

TG was employed to measure the mass loss and the derivative mass loss of pristine PVA and co-milled powder. The TG data were then introduced to Kissinger [30] and Ozawa [31] equations to investigate the thermal decomposition kinetics. Using mathematical deduction, decomposition reaction energy can be estimated, and reaction mechanism and influencing factors can be judged, thus providing a theoretical basis for material processing. The thermal decomposition rate can be expressed as

$$\frac{d\alpha}{dt} = Ae^{-E/RT}(1-\alpha)^n \quad (1)$$

or

$$\frac{d\alpha}{dt} = \frac{A}{\phi} e^{-E/RT}(1-\alpha)^n \quad (2)$$

where A is frequency factor, n reaction order, E activation energy, ϕ heating rate ($\phi = dT/dt$), $d\alpha/dt$ the rate of mass loss, and α is the fractional decomposition at any time. In this article, we use Kissinger and Ozawa methods to study the thermal decomposition kinetics of PVA/OMMT nanocomposites and calculate activation energy E at the highest mass loss peak. Figure 8 shows TG patterns of PVA and PVA/OMMT2 nanocomposites at different heating rates.

Kissinger method [30, 32]. Kissinger derived a useful expression that allows the calculation of activation energy by the temperature, because the maximum rate occurs when $d^2\alpha/dt^2 = 0$, which is expressed as

$$\ln\left(\frac{\beta}{T_{Pi}^2}\right) = \ln\left(\frac{AE}{g(\alpha)R}\right) - \frac{E}{RT_{Pi}} \quad (3)$$

Fig. 9 Kinetics of thermal decomposition of PVA and nanocomposites by using Kissinger equation

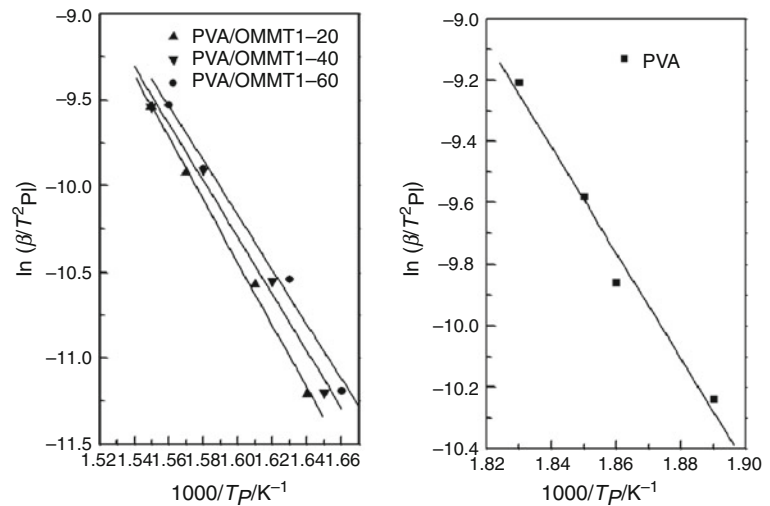


Table 2 Characteristics of TG kinetic data of PVA and PVA/OMMT2 by using Ozawa and Kissinger equations

Samples	$E/\text{kJ mol}^{-1}$	
	Ozawa method	Kissinger method
PVA	130.2	127.3
PVA/OMMT2-20	147.2	144.7
PVA/OMMT2-40	139.9	137.2
PVA/OMMT2-60	133.2	129.8

a linear plot of $\ln(\beta/T_p^2)$ versus $1000/T_p$ is obtained in Fig. 9. E and A can be calculated from slope and intercept. From Fig. 9 and Table 2, it is evident that E increases remarkably after co-milling.

Ozawa method [31, 32]. The Ozawa method essentially assumes that A and E are independent of T , whereas A and E are independent of α . The Ozawa equation is an integrated method. According to Doyle approximation, Ozawa equation is expressed as

$$\lg \beta = \lg(AE/RF(\alpha)) - 0.4567(E/RT) - 2.315 \quad (4)$$

where α is mass loss rate, for a specified α , $F(\alpha)$ is a constant, therefore a linear plot of $\log \beta$ versus $-1/T$ is obtained in Fig. 10, the slope is equal to $-0.4567E/R$, therefore E is calculated. Activation energy E obtained from both methods is listed in Table 2. Activation energy obtained from Ozawa and Kissinger methods is approximate, and activity energy of co-milling powder is obviously higher than pristine PVA, this conclusion is consistent with PA6/TPU/clay nanocomposite thermal behavior studied by Stankowski et al. [33]. These results provide a theoretical basis and further confirm the increased thermal stability

of intercalated structure of PVA/OMMT nanocomposites obtained through pan-milling.

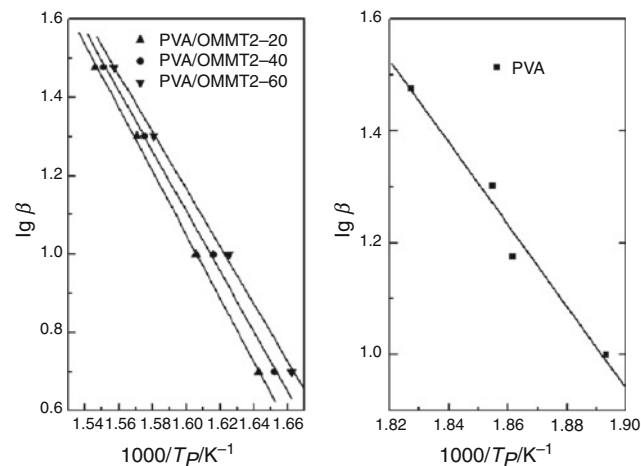
Conclusions

The results described above indicate that PVA/OMMT nanocomposite can be fabricated by co-milling the materials using our self-designed pan-mill which has shown a great potential for making well-dispersed PLS nanocomposites with improved thermal stability. XRD patterns illustrated that the interlayer spacing of OMMT1 increased to 3.45 nm, and that of OMMT2 increased to 4.55 nm. Better thermal stability is achieved for PVA/OMMT composites as proved by TG. After co-milling of 20 cycles, the starting decomposition temperatures of PVA/OMMT1 and PVA/OMMT2 powder increased by nearly 70 and 90 K, respectively. Thermal decomposition kinetics further confirms the increase in thermal stability. XRD and TEM consistently show that these samples have a hybrid structure where both intercalated and exfoliated silicate layers coexist. High hydrophilicity OMMT is proved to be favorable for producing intercalated structure. In summary, compared with the present common in situ intercalation polymerization, pre-polymer solution intercalation method, and polymer melting method, the solid-state pan-milling technique can more easily realize homogeneous dispersion of OMMT at nanometer level in polymer matrix. This solvent-free method is environmentally benign and quite efficient in productivity, exhibiting a promising potential for industrial application.

Acknowledgements The authors would like to thank National Science Foundation of China (50833003) for financial Support, and thank Analytical and Testing Center of Sichuan University for providing XRD measurement facility.

References

- Le Baron PC, Wang Z, Pinnavaia TJ. Polymer-layered silicate nanocomposites: an overview. *Appl Clay Sci*. 1999;15:11–29.
- Giannees EP. Polymer layered silicate nanocomposites. *Adv Mater*. 1996;8:29–35.
- Ray SS, Okamoto M. Polymer/layered silicate nanocomposites: a review from preparation to processing. *Prog Polym Sci*. 2003;28:1539–641.
- Zeng QH, Yu AB, Lu GQ, Paul DR. Caly-based polymer nanocomposites: research and commercial development. *J Nanosci Nanotechnol*. 2005;5:1574–92.
- Tjong SC. Structural and mechanical properties of polymer nanocomposites. *Mater Sci Eng*. 2006;53:73–197.
- Ray SS, Bousmina M. Biodegradable polymers and their layered silicate nanocomposites: in greening the 21 st century materials word. *Prog Mater Sci*. 2005;50:962–1079.
- Alexandre M, Dubois P. Polymer-layered silicate nanocomposites: preparation, properties and uses of a new class of materials. *Mater Sci Eng*. 2000;28:1–63.

**Fig. 10** Kinetics of thermal decomposition of PVA and nanocomposites by using Ozawa method

8. Ray SS, Yamada K, Okamoto M, Fujimoto Y, Ogami A, Ueda K. New polylactide/layered silicate nanocomposites. 5. Designing of materials with desired properties. *Polymer*. 2003;44:6633–44.
9. Chow WS, Lok SK. Thermal properties of poly(lactic acid)/organo-montmorillonite nanocomposites. *J Therm Anal Calorim*. 2009;2:627–32.
10. Ray SS, Okamoto K, Okamoto M. Structure-property relationship in biodegradable poly(butylene succinate)/layered silicate nanocomposites. *Macromolecules*. 2003;36:2355–67.
11. Gao F, Chen S, Hull JB. Layer expansion of layered silicates in solid polymer matrices by compression. *J Mater Sci Lett*. 2001;20:1807–10.
12. Lu D, Pan SW. Effects of ball milling dispersion of nano-SiO_x particles on impact strength and crystallization behavior of nano-SiO_x-poly(phenylene sulfide) nanocomposites. *Polym Eng Sci*. 2006;46:820–5.
13. Liang M, Lu CH, Huang YG, Zhang CS. Morphological and structural development of poly(ether ether ketone) during mechanical pulverization. *J Appl Polym Sci*. 2007;106:3895–902.
14. Zhang W, Zhang XX, Liang M, Lu CH. Mechanochemical preparation of surface-acetylated cellulose powder to enhance mechanical properties of cellulose-filler-reinforced NR vulcanizates. *Compos Sci Technol*. 2008;68:2479–84.
15. Zhao B, Lu CH, Liang M. Solvent-free esterification of poly(vinyl alcohol) and maleic anhydride through mechanochemical reaction. *Chin Chem Lett*. 2007;18:1353–6.
16. Zhang W, Liang M, Lu CH. Morphological and structural development of hardwood cellulose during mechanochemical pretreatment in solid state through pan-milling. *Cellulose*. 2007;14:447–56.
17. Xu X, Wang Q, China Patent ZL95111258.9, 1995.
18. Wang Q, Cao JZ, Huang JG, Xu XA. Study on the pan-milling process and the pulverizing efficiency of pan-mill type equipment. *Polym Eng Sci*. 1997;37:1091–101.
19. Chen Z, Wang Q. Pan-milling mixing—a novel approach to forming polymer blends and controlling their morphology. *Polym Int*. 2001;50:872–966.
20. Shao WG, Wang Q, Ma H. Study of polypropylene/montmorillonite nanocomposites prepared by solid-state shear compounding (S3C) using pan-mill equipment: the morphology of montmorillonite and thermal properties of the nanocomposites. *Polym Int*. 2005;54:336–41.
21. Shao WG, Wang QWF, Chen YH. Polyamide-6/natural clay mineral nanocomposites prepared by solid-state shear milling using pan-mill equipment. *J Polym Sci B Polym Phys*. 2006;44:249–55.
22. Shao WG, Wang Q, Li KS. Intercalation and exfoliation of talc by solid-state shear compounding (S3C) using pan-mill equipment. *Polym Eng Sci*. 2005;45:451–7.
23. Shao WG, Wang Q. Partial exfoliation and layer expansion of vermiculite layer in solid state by solid state shear milling (S3M). *J Appl Polym Sci*. 2006;101:1806–9.
24. Strawhecker KE, Manias E. Structure and properties of poly(vinyl alcohol)/Na⁺ montmorillonite nanocomposites. *Chem Mater*. 2000;12:2943–9.
25. Yürütü C, İşçi S, Ünlü C, Alçıl O, Ece ÖI, Güngör N. Preparation and characterization of PVA/OMMT composites. *J Appl Polym Sci*. 2006;102:2315.
26. Yang CC, Lee YJ, Yang JM. Direct methanol fuel cell (DMFC) based on PVA/MMT composites polymer membranes. *J Power Sources*. 2009;188:30–7.
27. Gopakumar TG, Lee JA, Kontopoulou M, Parent JS. Influence of clay exfoliation on physical properties of montmorillonite/polyethylene composites. *Polymer*. 2002;43:5483–91.
28. Lertwimolnun W, Vergnes B. Influence of compatibilizer and processing conditions on the dispersion of nanoclay in a polypropylene matrix. *Polymer*. 2005;46:3462–71.
29. Wakabayashi K, Pierre C, Dikin DA, Ruoff RS, Ramanathan T, Brinson LC, Torkelson JM. Polymer-graphite nanocomposites: effective dispersion and major property enhancement via solid-state shear pulverization. *Macromolecules*. 2008;41:1905–8.
30. Kissinger HE. Reaction kinetics in differential thermal analysis. *Anal Chem*. 1957;29:1702–6.
31. Ozawa T. Kinetic analysis of derivative curves in thermal analysis. *J Therm Anal*. 1970;2:301–24.
32. Lee JY, Shim MJ, Kim SW. Thermal decomposition kinetics of an epoxy resin with rubber-modified curing agent. *J Appl Polym Sci*. 2001;81:479–85.
33. Stankowski M, Kropidowska A, Gazda M, Haponiuk JT. Properties of polyamide 6 and thermoplastic polyurethane blends containing modified montmorillonites. *J Therm Anal Calorim*. 2008;3:817–23.